Journal of Engineering Physics and Thermophysics, Vol. 75, No. 2, 2002

SPECTROPHOTOMETRIC METHOD OF DIAGNOSING LIQUID-FUEL ROCKET ENGINES

Yu. M. Golovin, F. S. Zavelevich, A. P. Kuchin, Yu. P. Matsitskii, K. B. Moshkin, and A. S. Romanovskii

UDC 535.241+629.7.036.54-63

A method and equipment for optical diagnostics of liquid-fuel rocket engines (LR) is described. Experimental data on minimum detactable concentrations of such metals as Fe, Al, Mn, and Ni in the plume have been obtained. The radiation spectra of the plume of the engines of stages II and III of the Proton carrier rocket (CR) and of the full-scale oxygen-kerosene LR have been measured.

Introduction. At the present time, there are a fairly large number of methods for diagnosing units and assemblies of liquid-fuel rocket engines. They rely on measurement of the basic parameters of engines in the process of their testing by means of measuring equipment (pressure transducers, temperature sensors, flowmeters, vibration transducers, etc.), which complicates the carrying out of tests due to the introduction of changes into the units and assemblies of the engine and in a number of cases is prohibitive because of the possible change in the engine characteristics.

The method of plume radiation spectrum diagnostics of LRs has apparent advantages over the conventional methods. First, it does not require any changes in the propulsion system. Second, because of the small inertia, it provides the possibility of obtaining information in real time and, if necessary, taking adequate measures. Third, it enables one to judge the erosion of the LR parts and units by the emission lines of metals which can be determined by other methods. Monitoring of the carry-over of materials is extremely important not only for estimating the service life of different LR elements, but, in the first place, for solving the problem of preventing ignition.

The idea of determining the content of various chemical elements in the flowing jet of the working gas by the plume radiation spectrum and using these data for LR diagnostics has been developed in the last few years [1, 2].

Calculated Relations. Detection of traces of metals in the LR plume by the emission lines and determination of their concentration is not a trivial task. A number of factors impede the separation of metal lines and measurement of their intensity: molecular bands of combustion products, background continuous radiation, environment absorption, etc.

The intensity of the nonreabsorbed line J in an isothermal equilibrium flame with thickness L at temperature T is determined by the relation

$$J = NLAghc \exp\left[-E/(kT)\right]/(4\pi\lambda n) . \tag{1}$$

Relation (1) holds only for an optically thin emitter where the optical thickness

$$\tau = Ag\lambda^4 NL/(n8\pi c\Delta\lambda) \tag{2}$$

is less than unity.

Expression (2) holds for the majority of lines with a lower ground level. Table 1 presents the limiting values of NL for strong lines of some metals with the use of the data of [3].

The condition given by (2) is fulfilled, for example, for the engines of stages II and III of the Proton carrier rocket at a mass concentration of Fe $\leq 10^{-7}$.

Federal State Unitary Enterprise "M. V. Keldysh Research Center," Moscow, Russia; email: kerc@elnet.msk.ru. Translated from Inzhenerno-Fizicheskii Zhurnal, Vol. 75, No. 2, pp. 171–176, March–April, 2002. Original article submitted August 24, 2001.

 1062-0125/02/7502-0484$27.00

TABLE 1. Limiting Values of *NL* for Strong Lines of Some Metals

Metal	Wavelength λ, nm	$Ag \cdot 10^8$, sec^{-1}	*N*, m^{-3}	Doppler halfwidth of the line Δλ, nm	*NL*, m^{-2}
Al	396	1.3	5.9	$3 \cdot 10^{-3}$	$4 \cdot 10^{16}$
Cr	425	2.0	10.6	$2.3 \cdot 10^{-3}$	$3 \cdot 10^{16}$
Cu	324	4.1	2.4	$1.6 \cdot 10^{-3}$	$0.65 \cdot 10^{16}$
Fe	372	2.5	28.5	$2 \cdot 10^{-3}$	$9 \cdot 10^{16}$

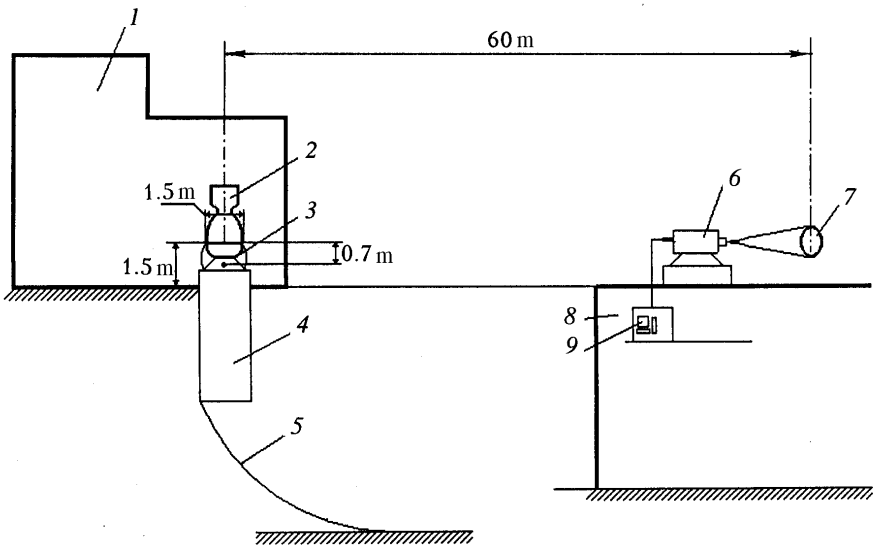

Fig. 1. Scheme of testing on the full-scale engine: 1) test bed; 2) engine; 3) Mach disk; 4) light-masking tube; 5) ray; 6) monochromator; 7) spherical mirror; 8) tester; 9) personal computer.

Measuring Equipment. The measuring equipment developed by us for measuring the radiation spectra of the LR plume [4] comprises an optical system, a diffraction monochromator, a photodetector unit, a video blaster, and a personal computer (PC) (Fig. 1).

In measurements, we used various optical systems. On the experimental plant with a model engine, to construct a plume image at the entrance slit of the monochromator, a quartz condenser 55 mm in diameter with a focal length of 70 mm was used. In testing the engines of the carrier rocket "Proton" and the oxygen-kerosene engine, a focusing spherical mirror 120 mm in diameter with a focal length of 1.2 m was used for this purpose.

The MDR-23 monochromator incorporates a plane diffraction grating (1200 lines per mm) and two spherical mirrors with a focal length of 600 mm. The operating spectral region of the monochromator ranges from 300 to 1000 nm and the inverse linear dispersion is 1.3 nm/mm.

The photodetector unit comprises a CCD linear image (2048 elements; the size of an element is 14 × 14 μm; the spectral sensitivity range is 320–800 nm), a controller, and buffer operational amplifiers.

The video blaster is designed for transforming a video signal into a digital data flow that arrives at the PC for further processing and display. The video blaster incorporates a controller, a random-access memory, an analog-to-digital converter, and a comparator. The main characteristics of the equipment are as follows:

spectral range — 320 to 800 nm;

spectral range of a single measurement — 30 nm;

maximum spectral resolution — 0.02 nm;

rate of measurements — 3 to 100 spectra/sec.

The relative spectral sensitivity of the equipment is given in Fig. 2.

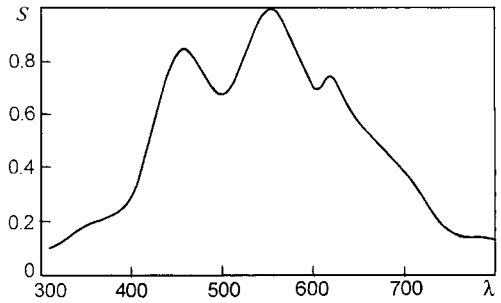

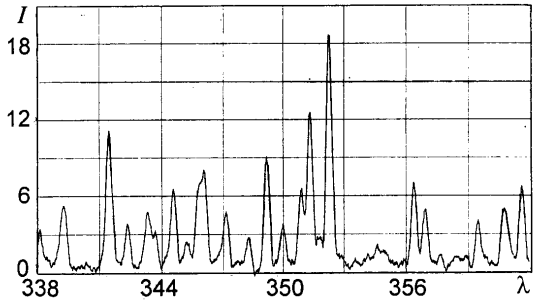

Fig. 2. Relative spectral sensitivity.

Fig. 3. Radiation spectrum of the plume on the model engine.

TABLE 2. Minimal Relative Concentrations C_{min} Registered on the Model Engine and Mass Flows G_{min}

Element	Salt	Wavelength λ, nm	C_{min}	G_{min}, g/sec
Cr	$K_2Cr_2O_7$	425.435	10^{-4}	0.01
Cu	$Cu(NO_3)_2$	510.554	10^{-4}	0.01
Fe	$FeSO_4.7H_2O$	385.991	$2.5\cdot10^{-4}$	0.025
Ni	$Ni(NO_3)_2$	352.454	$4\cdot10^{-4}$	0.04
Mn	$KMnO_4$	403.076, 403.307, 403.449	$6\cdot10^{-7}$	0.00006
K	$KMnO_4$	404.414, 404.72	$2\cdot10^{-6}$	0.0002

Experimental Plant. Imitation of the carry-over of small quantities of materials from the structural elements of the engine was performed by introducing into the combustion chamber small (1.3–15.0%) quantities of low-concentration solutions of salts and alkalis. To this end, we designed a special experimental plant [4] consisting of a model alcohol-oxygen LR and a dosing unit for feeding small quantities of low-concentration salt solutions into the combustion chamber. The solution was displaced from the dosing-unit vessel by high-pressure nitrogen. The flow rate of salt was controlled by the pressure differential in the vessel and the pipe-line of the fuel.

The main experiments on the model engine were performed with an overall fuel (oxygen + ethanol) flow rate of ~120 g/sec. The typical power conditions in testing were as follows: oxidizer flow rate — 82.25 g/sec; fuel flow rate — 39.6 g/sec; excess-oxidizer coefficient — 1.017; combustion-chamber pressure — 17.7 kg/cm^2; flow rate of salt solution — 1–15 g/sec; relative (mass) content of the metal — $(2–15)\cdot10^{-4}$.

Experiments on the Model Engine. The aim of experiments on the model engine was to determine the metal vapor sensitivity of the instrumentation in conditions close in the chemical composition of the plume to the full-scale ones. The instruments were tuned to the near-nozzle region of the plume, where the calculated temperature was 2200–2400 K and the pressure was equal to 0.1 MPa. The width of the entrance slit of the monochromator was assumed to be 0.15 mm to provide a spectral resolution of 0.2 nm.

Figure 3 shows, as an example, the radiation spectrum of the model engine plume in injecting a 12% solution of $Ni(NO_3)_2$ into its combustion chamber. In so doing, the Ni content in the jet was $1.5\cdot10^{-3}$. The spectra show a complete set of nickel lines, the most intense of which are the lines at 341.476, 346.165, 349.296, 351.034, and 352.454 nm.

The minimal relative concentrations C_{min} and mass flow rates G_{min} of various metals registered on the model engine are given in Table 2.

Experiments on Full-Scale LRs. Measurements of the radiation spectra of the plumes were made in testing two types of engines: a nitrogen tetroxide (NT) + nonsymmetric dimethylhydrosine (NDMH) engine and an oxygen + kerosene one.

The combustion products flowed out into open space, i.e., the jet was overexpanded. In testing the LR of the Proton carrier rocket, the instruments were tuned to the plume area at a distance of ~0.7 m from the nozzle exit section immediately behind the Mach disk, which was checked in video filming of the tests. The calculated temperature

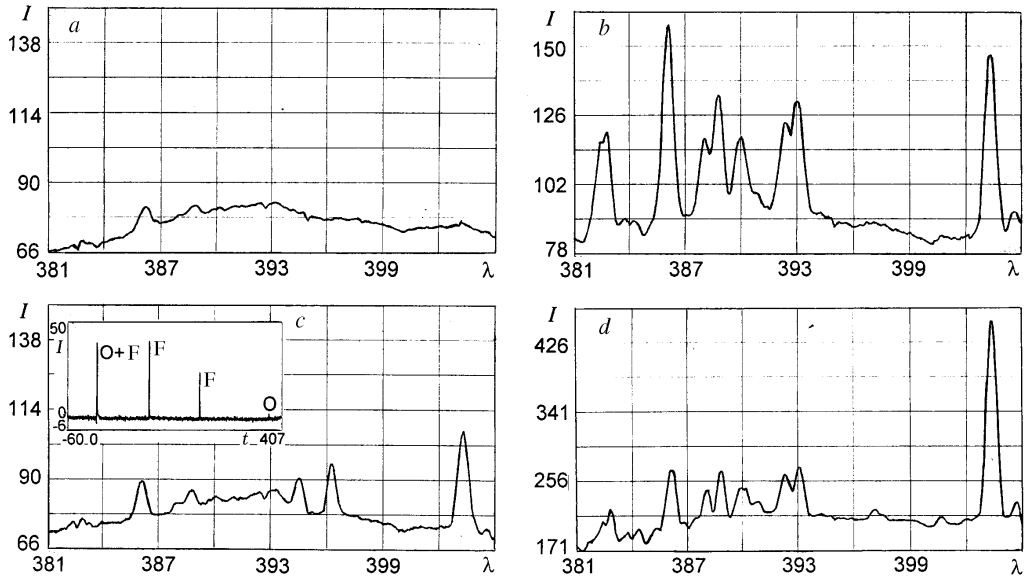

Fig. 4. Radiation spectrum of the engine: a) under standard power conditions; b) upon the introduction of steel into the fuel line; c) upon the introduction of aluminum into the fuel line; d) with scorching of the nozzle vanes. *I*, rel. units; λ, nm.

in this area under the condition of thermochemical equilibrium is ~3100 K and the pressure is ~0.2 MPa. In testing the oxygen-kerosene engine, the instruments were tuned to the plume area in the vicinity of the cylindrical nozzle exit section of the combustion chamber, since the Mach disk was inside the nozzle. The measurement rate in testing was 6 or 3 spectra per second. The width of the monochromator entrance slit was set at 0.2 mm, which provided a spectral resolution of 0.25 nm. The measurement data presented in Fig. 4 pertain to the LR of the Proton carrier rocket and those given in Fig. 5 — to the oxygen-kerosene engine.

Figure 4a shows a typical radiation spectrum of the plume characteristic of standard power conditions. Throughout the test the spectrum does not undergo any marked changes except for the moments of throwing-in of foreign particles and engine starting. Against the background of continuous radiation, two strong lines of iron at 385.99 and 388.63 nm stand out sharply. The radiation intensity in the lines does not change with time, which points to a constant flow rate of iron. The most probable cause of the appearance of iron in the plume is its presence in the propellant, which is corroborated by the results of the chemical analysis performed before each test. The mass content of Fe in the fuel before the given test was measured to be $\sim 4 \cdot 10^{-7}$ (its mass content in the propellant is $\sim 10^{-7}$), which corresponds to a flow rate of ~20 mg/sec.

Figure 4b gives the radiation spectrum of the plume upon the introduction into the fuel line of 2.5 g of 18KhN10T steel (70% Fe, 18% Cr, 10% Ni, and 1 to 2% Mn). From a comparison of the results presented in Fig. 4a and b it is seen that there is a sharp increase in the radiation intensity in the Fe lines at 385.99 and 388.63 nm and new lines of Fe at 382.59, 388.0, 389.97, 392.29, and 392.79 nm and of Mn at ~403.3 nm have appeared.

Interestingly, a more than 100-fold increase in the iron concentration increases the intensity of the strong lines of iron at 385.99 and 388.63 nm only by a factor of about ten. This is due to the self-absorption in the central part of the lines. This is corroborated by the value of *NL* calculated from the Fe flow rate. It appeared to be equal to $NL = 3 \cdot 10^{19}$ m^{-2} and is two orders of magnitude larger than the *NL* value at which relation (1) holds (see Table 1). In this case, with the Lorentz profile of the line the radiation intensity is proportional to the square root of the radiating component concentration.

The relative content of Cr atoms at a temperature of 3100 K at thermochemical equilibrium is measured to be only ~3%. Therefore, in this spectral region the intensity of the relatively strong lines of Cr (385.22, 385.52, and 388.68 nm) are masked by the intense Fe lines because of the insufficiently high spectral resolution.

The relative content of Ni atoms is ~0.85. The 385.83-nm line of Ni is masked by the strong 385.99-nm line of Fe. The 378.35- and 380.7-nm lines of Ni are present in the spectrum. In another spectral range (350–380 nm)

TABLE 3. Minimal Detectable Relative Concentrations C_{min} and Mass Flows G_{min} for the Engines of Stages II and III of the Proton Carrier Rocket

Element	Wavelength λ, nm	C_{min}	G_{min}, g/sec
Al	394.4, 396.15	$5\cdot10^{-7}$	0.1
Fe	371.99, 373.6, 374.8, 385.99, 388.63	$5\cdot10^{-8}$	0.01
Ni	352.454, 361.94	$1\cdot10^{-8}$	0.002
Mn	403.08, 403.31, 403.45	$3\cdot10^{-9}$	0.0006

nickel lines are also observed under standard power conditions without throwing-in of powders. In these spectra, one can see Ni lines at 352.45 and 361.94 nm and Fe lines at 371.9, 373.6, and 374.8 nm. It is likely that small inclusions of these metals in the propellant, whose relative mass concentrations are $\sim10^{-7}$ for Fe and $\sim10^{-8}$ for Ni, are registered.

Figure 4c shows the radiation spectrum of the plume upon the introduction of 700 mg of powder of AMg6 aluminum alloy containing 0.5 to 0.8 mass percent of Mn. The powder was introduced into the fuel line. About 20% (mass) of the largest particles were retained by the filters and did not get into the combustion chamber and, consequently, into the plume. As seen from the results presented, upon the introduction of powder, radiation arises in the Al lines at 394.4 and 396.15 nm and in the Mn lines at ~403.3 nm (this is a superposition of the Mn lines at 403.076, 403.307, and 403.449 nm).

In other experiments, AMg6 powder was introduced on the oxidizer line. Because of the AMg6 powder oxidation, the concentration of Al and Mn atoms and, consequently, the radiation intensity in the Al and Mn lines were much lower than those presented in Fig. 4c.

The upper part of Fig. 4c shows the time dependence of the radiation in the Al line with a center at 396.15 nm. The radiation peaks approximately correspond to the moment of introduction of AMg6 particles. Indices O and F indicate on what line (oxidizer or fuel) particles are introduced.

Luminescence in the Al and Mn lines is observed for ~1 sec. This means that the registered radiation intensity corresponds to a flow rate of Al of ~600 mg/sec and of Mn ≈ 4 mg/sec or to a relative mass concentration of $3\cdot10^{-6}$ and $2\cdot10^{-8}$, respectively. In fact, only a small portion of the source material is contained in the plume in the form of atoms forming the spectral lines. For instance, at thermochemical equilibrium behind the Mach disk at T = 3100 K only 3% of Al and 50% of Mn are contained in the form of atoms.

The presence of inclusions of Fe with a known concentration and of Ni in the propellant, the introduction into the propellant of normalized weights of powders from steel and aluminum alloy AMg6, and the results of the experiments on the model engine have enabled us to estimate the smallest detectable relative concentrations C_{min} and the mass flow rates G_{min} of various metals in the plume of these engines (Table 3).

The spectrophotometric method of diagnostics has proved to be highly efficient in the real-time registration of deviations from the normal behavior of the engine, which are not observed, as a rule, with the use of conventional methods.

In starting the engine, during the first ~4 sec in the plume radiation spectra, Mn lines are always observed and often Ca (396.85 nm) lines and a heightened content of Fe are noted. This is likely to be due to the removal of contaminants from the intraengine cavities.

At a stop or under certain power conditions, in the plume spectrum CN bands (388.34, 386.19, and a weaker band at 387.14 nm) appear, which is likely to be due to the incomplete propellant combustion.

Interesting spectra were obtained in the first ~20 sec of one of the tests of the stage III engine of the Proton carrier rocket (Fig. 4d). In the spectrum, a powerful line radiation in the region of 403.2 nm is seen. It is caused by the superposition of the Mn lines at 403.08, 403.31, and 403.45 nm. The other spectral features pertain, most probably, to the iron lines at 382.04, 382.59, 388, 388.62, 389.97, 392.29, 392.79, 393.03, and 396.93 nm. The spectrum (see Fig. 4d) is very similar to that given in Fig. 4b, where 2.5 g of steel were introduced into the fuel line. The intensity of the Fe lines is approximately the same. However, the background radiation is twice that registered upon the introduction of 2.5 g of steel. This can be explained by the appearance of solid and/or liquid particles of metal oxides.

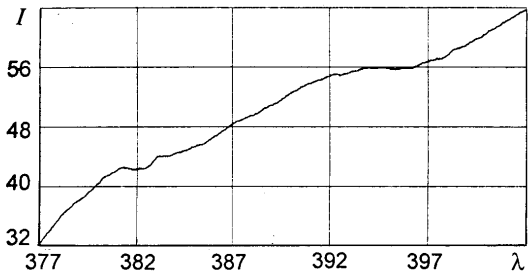

Fig. 5. Radiation spectrum of the oxygen-kerosene engine.

In the course of time, the line intensity decreased and after ~30 sec only the 385.99- and 388.63-nm iron lines are clearly seen in the spectra, as in Fig. 4a.

Such a behavior of the plume radiation spectra is likely to be due to the carry-over of steel at a flow rate of 2 g/sec caused by the burning of some of the engine elements in the first few seconds of testing.

The inspection for likely defects conducted after the testing has shown that a considerable scorching of some of the nozzle vanes of the turbo-driven pump assembly takes place. It is important to note that this event was not revealed by the traditional methods in checking the flow rates, pressures, temperatures, and vibrations.

We did not reveal any considerable influence of the introduction of particles on the steel carry-over at the instant the particles were injected. The appearance of through lick-outs of the combustion chamber wall was accompanied by an increase in the radiation in the CN bands.

The character of the plume radiation spectrum of the oxygen-kerosene engine (Fig. 5) greatly differs from the plume spectra of engines burning the propellant N_2O_4 + $((CH_3)_2N_2H_2)$. While for the Proton carrier rocket engines the background radiation is mainly a superposition of numerous molecular bands, the character of the oxygen-kerosene engine spectra is well explained by the radiation of solid particles (soot particles) in the exhaust jet.

The background radiation of the oxygen-kerosene engine plume in the absence of changes in the power conditions changes very slightly with time up to the moment the engine is shut down, when the radiation sharply (by a factor of ~3) increases and after another ~1 sec fades out. The most probable cause of the sharp increase in radiation is the increase in the soot concentration under the transient conditions of "stopping."

In the plume radiation spectrum of the oxygen-kerosene engine, at certain instants of time lines of some elements were observed. For instance, a heightened content of Al is observed at the very beginning of the testing for ~10 sec. Afterwards Al does not appear in the spectra. This is likely to be due to the operation of the starting powder engine whose combustion products contain aluminum in their composition. We did not detect the presence of iron in the jet throughout the testing.

Conclusions. The measurements of the plume radiation spectra in the process of fire testing of full-scale LRs have demonstrated a high efficiency of the spectrophotometric method of diagnostics. As a result, we managed to detect the presence of Fe and Ni inclusions in the propellant, register the throwing-in of weights of aluminum alloy and steel powders into the propellant lines, register and follow the ignition of the turbo-driven pump assembly nozzle set in testing one of the engines and the evolution of erosion processes associated with the burn-out of the injectors of the combustion chamber head and the appearance of lick-outs and burn-outs in the nozzle critical section, detect the presence of impurities in the propellant lines in the first few seconds after the appearance of the plume, etc.

The set of experiments performed with the use of high-speed spectrum equipment on a model LR burning oxygen + ethanol components, on the Proton carrier rocket engines of stages II and III, and on a full-scale oxygen-kerosene engine permit the following conclusions:

1. The method and equipment developed by us permit real-time check of the carry-over of materials from the structural elements of the LR in the process of fire testing.

2. Prerequisites have been created for detecting "precursors" of LR ignition (a sharp increase in the rate of carry-over of materials) at early stages of evolution of the process, where it is still possible to prevent catastrophic consequences.

3. The method makes it possible to investigate practically high-temperature gas jets.

NOTATION

J, nonreabsorbed line intensity, W/(m^2·sr); N, volume concentration, m^{-3}; L, flame thickness, m; A, transition probability, sec^{-1}; g, statistical weight; n, state sum; E, upper level energy, eV; λ, wavelength, nm; T, temperature, K; V, velocity of light, m/sec; h, Planck constant, J·sec; k, Boltzmann constant, eV/K; $\Delta\lambda$, spectral line halfwidth, nm; τ, optical thickness; $C_{\min}$, minimal relative concentration; $G_{\min}$, minimal mass flow, g/sec; S, relative spectral sensitivity; t, time, sec.

REFERENCES

1. G. D. Tejwani, F. E. Bircher, D. B. Van Dyke, and C. C. Thurman, *J. Spac. Rock.*, No. 3, 387–394 (1998).
2. D. A. Benzing and K. W. Whitaker, *J. Spac. Rock.*, No. 6, 830–836 (1998).
3. C. Corliz and Y. Bozman, *Transition Probabilities and Strengths of Oscillators of 70 Elements* [Russian translation], Moscow (1968).
4. F. S. Zavelevich, Yu. M. Golovin, Yu. P. Matsitskii (Matsitsky), K. B. Moshkin, and A. S. Romanovskii (Romanovsky), in: *Proc. 4th Int. Symp. on Liquid Space Propulsion: Scientific Progress in the Service of Space Access at the Beginning of the Third Millenium*, DhR-Lampoldshausen, Germany, March 13–15, 2000 (2000).